Structures of the Cu(I) and Cu(II) Forms of Amine Oxidases from X-ray Absorption Spectroscopy

David M. Dooley,*,† Robert A. Scott,*,§ Peter F. Knowles,‡ Christopher M. Colangelo,§ Michele A. McGuirl,† and Doreen E. Brown†

Contribution from the Department of Chemistry and Biochemistry, Montana State University, Bozeman, Montana 59717-0340, the Center for Metalloenzyme Studies, University of Georgia, Athens, Georgia 30602-2556, and the Department of Biochemistry and Molecular Biology, University of Leeds, Leeds LS2 9JT, United Kingdom

Received January 29, 1997. Revised Manuscript Received October 14, 1997

Abstract: X-ray absorption spectroscopy has been used to define the copper-site structures in both the resting (oxidized) and dithionite-reduced states of amine oxidases from bovine plasma, porcine plasma, porcine kidney, pea seedlings, and the gram-positive bacterium *Arthrobacter* P1. The Cu(II) EXAFS data are consistent with four first-shell N,O scatterers (three of which are imidazoles) at a distance of 1.98−2.00 Å for all five amine oxidases. These scatterers are assigned as the equatorial ligands. Because the raw Cu(II) EXAFS data are essentially identical for all the enzymes examined, the crystallographically defined Cu(II) sites of the pea seedling and *E. coli* amine oxidases are excellent models for the copper sites in the mammalian enzymes. Analysis of the K-edges and EXAFS data for the reduced amine oxidases indicates that the Cu(I) sites are three-coordinate, with at least two imidazoles; the range for the bond distances among the reduced enzymes is 1.94−1.99 Å. Therefore, the results are consistent with a decrease in coordination number from five (or, possibly six) to three upon reduction of Cu(II) to Cu(I). Three-coordinate Cu(I) complexes with predominately N,O ligands generally react with dioxygen, suggesting that the Cu(I) sites in amine oxidases may serve this role in catalysis.

Introduction

Copper-containing amine oxidases have emerged as a new type of metalloenzyme characterized by (1) the presence of a novel protein-derived redox cofactor, topa quinone (TPQ), which is produced by post-translational modification of an invariant tyrosine residue, and (2) the probable participation of a semiquinone radical, Cu(I)−TPQ$^{\bullet}$, in catalytic turnover.[1−4] These enzymes catalyze the oxidative deamination of primary amines, a two-electron oxidation using molecular oxygen as the oxidant (eqs 1 and 2).

$$E + RCH_2NH_2 \rightleftharpoons E{\cdot}RCH_2NH_2 \rightarrow E_{red} + RCHO \quad (1)$$

$$E_{red} + O_2 \rightarrow E + H_2O_2 + NH_3 \quad (2)$$

Substrate amines reduce the TPQ cofactor in the first phase (eq 1) via a general base-catalyzed abstraction of H^+ from the primary amine methylene group (Scheme 1).[5] Two species are present in the substrate-reduced enzyme (E_{red}) that are in temperature-dependent equilibrium (**4** ⇌ **5**, Scheme 1).[6] Previous work suggests that the magnitude of this equilibrium constant varies among amine oxidases, such that the Cu(I) semiquinone (**5**, Scheme 1) is readily detectable in some enzymes, but not in others.[6] The Cu(I) semiquinone is proposed to be the species that reacts with molecular oxygen. Temperature-jump relaxation measurements have shown that the Cu(I) semiquinone is formed at a catalytically competent rate from the Cu(II) aminoresorcinal form (**4**, Scheme 1) in both prokaryotic and eukaryotic amine oxidases.[7,8] Therefore it will be important to characterize the structures of the Cu(I) forms of amine oxidases.

X-ray crystal structures are available for two amine oxidases, from *Escherichia coli* (*E. coli*)[9] and pea seedlings,[10] in the resting (oxidized) state; the structure of the pea seedling amine oxidase Cu(II) site is shown in Figure 1. Although the coordination geometry appears somewhat distorted at the current resolution, it is well within the range typically observed for tetragonal Cu(II) complexes. The Cu(II) site structure is in

† Montana State University.
§ University of Georgia.
‡ University of Leeds.

(1) Klinman, J. P.; Mu, D. *Annu. Rev. Biochem.* **1994**, *63*, 299−344.
(2) McIntire, W. S.; Hartmann, C. In *Principles and Applications of Quinoproteins*; Davidson V. L., Ed.; Marcel Dekker: New York, 1993; pp 97−171.
(3) Knowles, P. F.; Dooley, D. M. In *Metal Ions in Biological Systems*; Sigel, H., Sigel, A., Eds.; Marcel Dekker: New York, 1994; Vol. 30, pp 361−403.
(4) Tanizawa, K. *J. Biochem (Tokyo)* **1995**, *118*, 671−678.
(5) (a) Farnum, M. F.; Palcic, M.; Klinman, J. P. *Biochemistry* **1986**, *25*, 1898−1905. (b) Hartmann, C.; Klinman, J. P. *Biochemistry* **1991**, *30*, 4605−4611. (c) Janes, S. M.; Klinman, J. P. *Biochemistry* **1991**, *30*, 4599−4605. (d) Hartmann, C.; Brzovic, P.; Klinman, J. P. *Biochemistry* **1993**, *32*, 2234−2241. (e) Medda, R.; Padiglia, A.; Pedersen, J. Z.; Rotilio, G.; Finazzi-Agrò, A. F.; Floris, G. *Biochemistry* **1995**, *34*, 16375−16381. (f) Steinebach, V.; De Vries, S.; Duine, J. A. *J. Biol. Chem.* **1996**, *271*, 5580−5588.
(6) Dooley, D. M.; McGuirl, M. A.; Brown, D. E.; Turowski, P. N.; McIntire, W. S.; Knowles, P. F. *Nature* **1991**, *349*, 262−264.
(7) Turowski, P. N.; McGuirl, M. A.; Dooley, D. M. *J. Biol. Chem.* **1993**, *268*, 17680−17682.
(8) Dooley, D. M.; Brown, D. E. *J. Biol. Inorg. Chem.* **1996**, *1*, 205−209.
(9) Parsons, M. R.; Convery, M. A.; Wilmot, C. M.; Yadav, K. D. S.; Blakeley, V.; Corner, A. S.; Phillips, S. E. V.; McPherson, M. J.; Knowles, P. F. *Structure* **1995**, *3*, 1171−84.
(10) Kumar, V.; Dooley, D. M.; Freeman, H. C.; Guss, J. M.; Harvey, I.; McGuirl, M. A.; Wilce, M. C. J.; Zubak, V. M. *Structure* **1996**, *4*, 943−955.

S0002-7863(97)00312-0 CCC: $15.00
Published on Web 02/26/1998

Scheme 1. Mechanism of Substrate Amine Oxidation

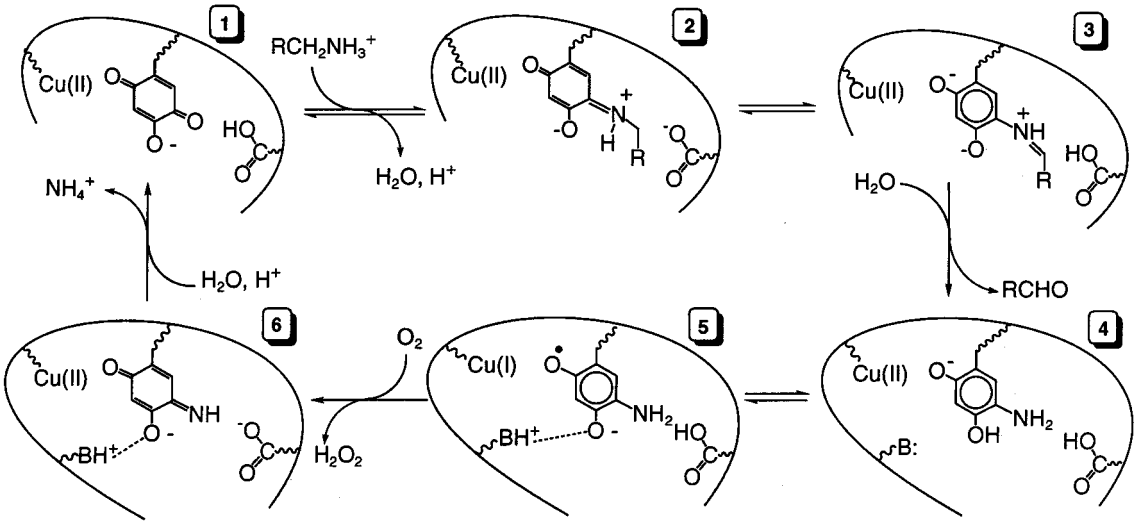

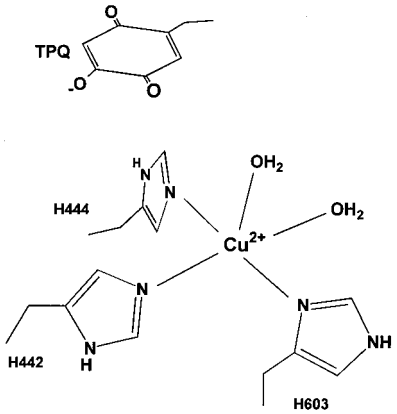

Figure 1. Schematic structure of the Cu(II) site of pea seedling amine oxidase. The active-site TPQ residue is also shown.

excellent agreement with results from spectroscopic studies,[11−14] including previous X-ray absorption spectroscopy (XAS) experiments,[11] which predicted a tetragonal geometry ($d_{x^2-y^2}$ ground state) with three coordinated histidine imidazoles and equatorial and axial water ligands. There are no hydrogen bonds from protein residues to the coordinated water molecules, indicating these waters may be labile, as established by solvent proton relaxation measurements.[13] Both model chemistry[15] and studies on other copper enzymes[16] indicate that the coordination number generally decreases upon reduction for copper centers which react with oxygen. Thus, three-coordinate Cu(I) sites may be expected to react with dioxygen in protein environments.

XAS, including extended X-ray absorption fine-structure (EXAFS) analysis, has been used to probe the Cu(II) coordination structures of amine oxidases from bovine and porcine plasma,[11] as well as the sulfide complex of the bovine plasma enzyme.[17] Here we report the structures of the reduced, Cu(I) forms of several amine oxidases, based on Cu K-edge and EXAFS data. Results on the corresponding oxidized forms of these amine oxidases are presented to permit systematic comparisons of the structural changes accompanying copper reduction.

Experimental Section

Amine oxidases from bovine plasma (BPAO),[18] porcine plasma (PPAO),[19] porcine kidney (PKAO),[20] pea seedlings (PSAO),[21] and the gram-positive bacterium *Arthrobacter* P1 (APAO)[22] were purified, assayed, and characterized by procedures described in the literature.[18−22] The specific activities and gel-electrophoretic behavior of all the amine oxidases were consistent with high purity (≥90−95% homogeneity on native or denaturing gels). Adventitious metal ions were removed prior to XAS experiments via extensive dialysis against metal ion-free buffer, or against buffers containing EDTA, followed by dialysis against buffer alone. Reduced amine oxidase samples were prepared by adding a minimum amount of freshly prepared, buffered dithionite solution under anaerobic conditions. Copper X-ray absorption edge and EXAFS data were collected at the Stanford Synchrotron Radiation Laboratory with the SPEAR ring operating at 3.0 GeV, 50−90 mA. Details of the data collection and reduction are summarized in Table 1. Standard EXAFS data reduction was performed[23] with EXAFSPAK software (courtesy of G. N. George). Both single- and multiple-scattering paths ≤4.5 Å from the Cu atom were used to identify and quantify imidazole coordination due to histidine residues. Multiple-scattering paths were built from the crystal structure coordinates of tetrakis(imidazole)copper-(II) sulfate.[24] The model was imported into Ball and Stick software (v3.5, Cherwell Scientific) and edited to contain only the copper and one imidazole. These coordinates were then imported into FEFF v.

(11) (a) Scott, R. A.; Dooley, D. M. *J. Am. Chem. Soc.* **1985**, *107*, 4348−4350. (b) Knowles, P. F.; Strange, R. W.; Blackburn, N. J.; Hasnain, S. S. *J. Am. Chem. Soc.* **1989**, *111*, 102−107.

(12) McCracken, J.; Peisach, J.; Dooley, D. M. *J. Am. Chem. Soc.* **1987**, *109*, 4064−4072.

(13) (a) Dooley, D. M.; McGuirl, M. A.; Coté, C. E.; Knowles, P. F.; Singh, I.; Spiller, M.; Brown, R. D., III; Koenig, S. H. *J. Am. Chem. Soc.* **1991**, *113*, 754−761. (b) Barker, R.; Boden, N.; Cayley, G.; Knowles, P. F. *Biochem. J.* **1979**, *177*, 289−302.

(14) Dooley, D. M.; Brown, D. E.; Clague, A. W.; Kemsley, J. N.; McCahon, C. D.; McGuirl, M. A.; Turowski, P. N.; McIntire, W. S.; Farrer, J. A.; Thomson, A. J. In *Bioinorganic Chemistry of Copper*; Karlin, K. D., Tyeklár, K., Eds.; Chapman & Hall: New York, 1993; pp 459−470.

(15) (a) Karlin, K. D.; Gultneh, Y. *Prog. Inorg. Chem.* **1987**, *35*, 219−227. (b) See the following for several discussions related to these points: *Bioinorganic Chemistry of Copper*; Karlin, K. D., Tyeklár, K., Eds.; Chapman & Hall: New York, 1993.

(16) (a) Klinman, J. P. *Chem. Rev.* In press. (b) Dooley, D. M. In *Encyclopedia Inorg. Chem.*, vol. 2, King, R. B., Ed., Wiley: Chichester, 1994; pp 905−924.

(17) Scott, R. A.; Coté, C. E.; Dooley, D. M. *Inorg. Chem.* **1988**, *27*, 3859−3861.

(18) BPAO was purified by minor modifications of the procedures described in ref 5c.

(19) Rius, F. X.; Knowles, P. F.; Pettersson, G. *Biochem. J.* **1984**, *220*, 767−772.

(20) Dooley, D. M.; McGuirl, M. A. *Inorg. Chim. Acta* **1986**, *123*, 231−236.

(21) McGuirl, M. A.; McCahon, C. D.; McKeown, K. A.; Dooley, D. M. *Plant Physiol.* **1994**, *106*, 1205−1211.

(22) McIntire, W. S. *Methods Enzymol.* **1990**, *188*, 227−235.

(23) Scott, R. A. *Methods Enzymol.* **1985**, *117*, 414−459.

(24) Fransson, G.; Lundberg, B. K. S. *Acta Chem. Scand.* **1972**, *26*, 3969−3976.

Table 1. X-ray Absorption Spectroscopic Data Collection and Reduction for Amine Oxidase Samples

	oxidized	reduced
SR facility	SSRL	SSRL
beamline	7−3/4−1	7−3/4−1
monochromator crystal	Si[220]	Si[220]
detection method	fluoresence	fluoresence
detector type	solid state array[a]	solid state array[a]
temp, K	4−30	4−80
energy standard	Cu foil (first inflection)	Cu foil (first inflection)
energy calibration, eV	8980.3	8980.3
E_0, eV	8990	8990
pre-edge background		
energy range, eV	8650−8945[b]	8650−8945[b]
Gaussian center, eV	8040	8040
width, eV	1000	1000
spline background		
energy range, eV	8990−9193 (4)	8990−9193 (4)
(order polynomial)	9193−9396 (4)	9193−9396 (4)
	9396−9600 (3)	9396−9600 (3)

[a] The 13-element Ge solid-state X-ray fluorescence detector at SSRL is provided by the NIH Biotechnology Research Resource. [b] Background was fitted in this region and then extrapolated to the whole data region. This background was then subtracted from the raw XAS data.

5.04 software[25−27] to calculate scattering amplitudes and phase shifts for each scattering path containing four or fewer segments. A constrained fitting process was then used in which coordination numbers were constrained to be integer, and the distances and Debye−Waller factors for outer-shell atoms of imidazole rings were constrained to a given ratio with first-shell (Cu−N) distances and Debye−Waller factors, respectively. First-shell distances are expected to be accurate to within ±0.02 Å.

Results

Cu K-edges for both the oxidized and dithionite-reduced forms of five amine oxidases are shown in Figure 2. The sets of edges among the oxidized states and also among the reduced states of all the amine oxidases are very consistent. The energy and shape of the oxidized edges are entirely consistent with Cu(II) sites with mixed N,O first-shell donors. Further, in the reduced samples, the shifts to lower energy and the appearance of the prominent transitions at ∼8985 eV are characteristic of Cu(I) K-edges.[28] Figure 3A displays the k^3-weighted EXAFS of the oxidized and reduced states of the five amine oxidases; Figure 3B displays the associated Fourier transforms (FTs) of these EXAFS data. Considering the data for the oxidized samples first, it is clear that the raw EXAFS and the major features of the FTs are closely similar among the amine oxidases examined. Comparisons of the raw EXAFS data and FTs for the reduced samples lead to a similar conclusion. Note that the EXAFS amplitude is significantly reduced in the Cu(I) forms compared to the amplitude of the Cu(II) forms (Figure 3). Since the EXAFS amplitude is related to the number of first-shell (N,O) scatterers, the reduced amplitude of the Cu(I) forms suggests that the coordination number of the amine oxidases decreases with chemical reduction. Kau et al. have established that the Cu(I) edge may be diagnostic of the coordination

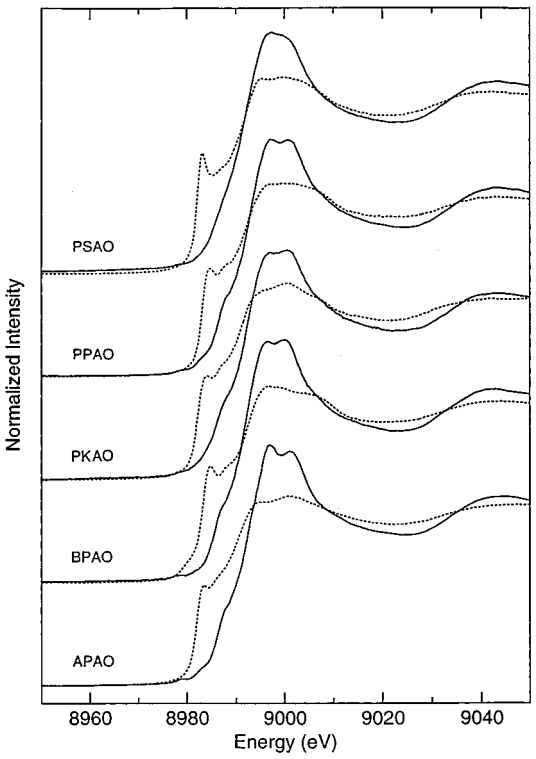

Figure 2. Copper K-edge X-ray absorption spectra of five amine oxidases: (—) oxidized forms and (- - -) dithionite-reduced forms.

number.[28] Comparisons of the amine oxidase Cu(I) edges with those of model compounds (not shown) indicates that all the amine oxidase Cu(I) sites are three-coordinate. Fits of the EXAFS data are shown in Figures 4 and 5 and summarized in Table 2. Very similar fitting parameters satisfactorily reproduce the key features of the data for all five amine oxidases. Initial curve-fitting of first-shell filtered data (Tables 1 and 2 in the Supporting Information) gave first-shell distances within ±0.02 Å and similar coordination numbers as the fits to the unfiltered data, so only the latter are presented in Table 2. Three imidazoles and one additional (N,O) ligand at 1.98−2.00 Å are present in the Cu(II) first-coordination shell. Note that in each case three imidazoles are required to fit the outer-shell FT peaks at $R' = 3$ and 4 Å (Figure 4B). Addition of a fifth ligand did not significantly improve the fits, as expected given that Cu(II) EXAFS is generally not very sensitive to the presence of axial N,O ligands. Fits of the reduced Cu(I) EXAFS data were less definitive owing to the lower signal-to-noise in these data. Inspection of the fitting results (Table 2) establishes that the lower signal-to-noise is a consequence of the decreased coordination number with only light (N,O) donors and significantly greater disorder, as measured by σ_{as}^2. In all cases the most reasonable fits were obtained with a three-coordinate geometry, with bond distances of 1.94−1.99 Å. However, only two imidazole rings appear to contribute to the outer-shell multiple scattering. Fits based on two-coordinate geometries with two N(imidazole) ligands were slightly worse (f' basis), or led to physically unreasonable values for σ_{as}^2. Fits based on three coordinated imidazoles were worse *and* had unreasonable σ_{as}^2 values, if the outer-shell scattering from all three was included. There is a greater spread among the Cu(I)−N(imidazole) distances than among the Cu(II)−N(imidazole) distances (Table 2). Accordingly, it is possible there is greater variability among the structures of the reduced enzymes, compared to the oxidized forms. Examination of Figure 5 might suggest that the fit for reduced APAO is somewhat worse than the fits for the other

(25) Rehr, J. J.; Albers, R. C. *Phys. Rev. B* **1990**, *41*, 8139−8149.
(26) Mustre de Leon, J.; Rehr, J. J.; Zabinsky, S. I.; Albers, R. C. *Phys. Rev. B*, **1990**, *44*, 4146−4156.
(27) Rehr, J. J.; Mustre de Leon, J.; Zabinsky, S. I.; Albers, R. C. *J. Am. Chem. Soc.* **1991**, *113*, 5135−5140.
(28) Kau, L.-S.; Spira-Solomon, D. J.; Penner-Hahn, J. E.; Hodgson, K. O.; Solomon, E. I. *J. Am. Chem. Soc.* **1987**, *109*, 6433−6442.

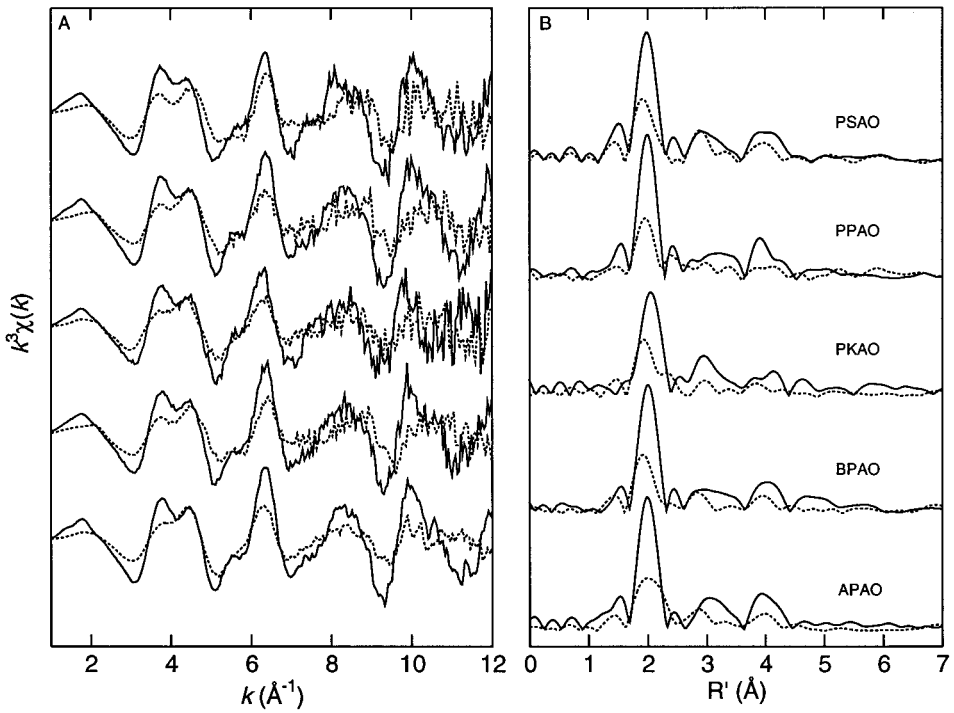

Figure 3. Amine oxidase EXAFS (A) and Fourier transforms (B): (—) oxidized forms and (- - -) dithionite-reduced forms. FTs were computed over the range $k = 2.0-12.0$ Å^{-1}, k^3-weighted, and were phase corrected by using Cu−N phase shifts.

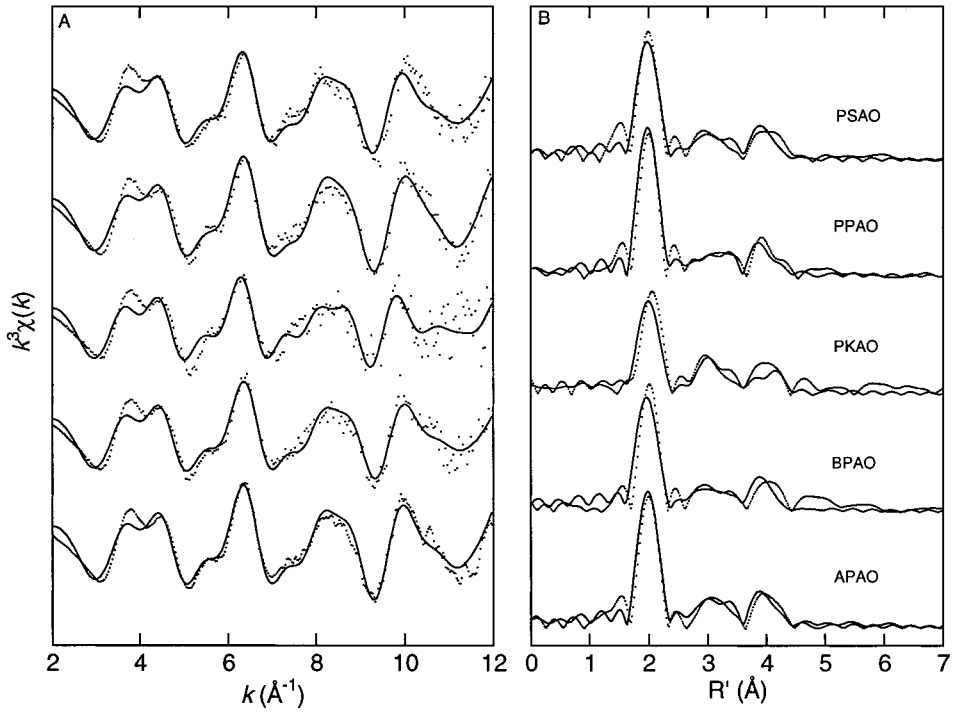

Figure 4. Comparison of the EXAFS data (A) and FTs (B) for oxidized amine oxidases with the corresponding fits from Table 2. Fits are shown as solid lines, the data as dots. These fits correspond to fits SAOA-06 (PSAO), PPOAB-06 (PPAO), PAOAD-06 (PKAO), BAOAC-06 (BPAO), and APOAB-06 in Table S1 (Supporting Information).

amine oxidases in the region of the major FT peak at ∼2 Å. On an f' basis this is not apparent (Table 2), as f' for APAO is not significantly different from the mean value of f' for the raw data, and barely outside the standard deviation from the mean for the smoothed data.

Discussion

EXAFS is rather insensitive to structural features beyond the first coordination sphere, so structural information is provided primarily for the closest, most strongly bound ligands. Nevertheless, the present data provide strong support for previous suggestions that the principal structural features of the copper sites among amine oxidases are conserved.[3,11−14] This conclusion, previously applicable only to the oxidized Cu(II) forms, may now be extended to the reduced Cu(I) states as well, at least at the level of the first coordination sphere. Further, the similarities of the EXAFS establish that the crystallographically determined PSAO Cu(II) coordination structure (Figure 1)[10] is

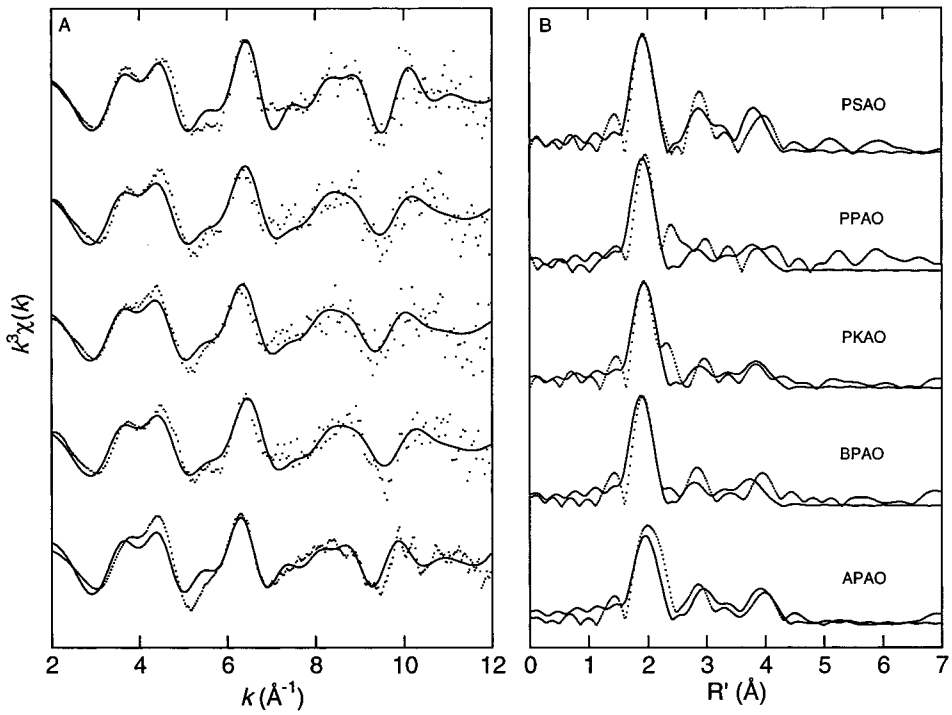

Figure 5. Comparison of the EXAFS data (A) and the FTs (B) for reduced amine oxidases with the corresponding fits from Table 2. Fits are shown as solid lines, the data as dots. These fits correspond to fits SADA-04 (PSAO), PPDAB-04 (PPAO), PADCD-04 (PKAO), BPABD-04 (BPAO), and APDC-04 (APAO) in Table S2 (Supporting Information).

Table 2. Curve-Fitting Results for Cu EXAFS of Amine Oxidases[a]

	oxidized							dithionite reduced						
sample	group	shell	N_s	R_{as} (Å)	σ_{as}^2 (Å^2)	ΔE_0 (eV)	f' [b]	group	shell	N_s	R_{as} (Å)	σ_{as}^2 (Å^2)	ΔE_0 (eV)	f'
pea seedling	imid + N/O	Cu−N	(4)[d]	1.98	0.0025	−0.31	0.080	imid + N/O	Cu−N	(3)	1.94	0.0061	−3.32	0.108
$k = 2.0-12.0$ Å^{-1}	imid	Cu−C_2	(3)	[2.97][e]	[0.0020]	[−0.31]	⟨0.064⟩[c]	imid	Cu−C_2	(2)	[2.91]	0.0020	[−3.32]	⟨0.070⟩
	imid	Cu−N_3	(3)	[4.12]	[0.0028]	[−0.31]		imid	Cu−N_3	(2)	[4.03]	[0.0027]	[−3.32]	
	imid	Cu−C_4	(3)	[4.15]	[0.0028]	[−0.31]		imid	Cu-C_4	(2)	[4.06]	[0.0028]	[−3.32]	
	imid	Cu−C_5	(3)	[3.01]	[0.0020]	[−0.31]		imid	Cu−C_5	(2)	[2.95]	[0.0020]	[−3.32]	
pig plasma	imid + N/O	Cu−N	(4)	1.98	0.0008	−0.19	0.072	imid + N/O	Cu−N	(3)	1.94	0.0065	−4.18	0.113
$k = 2.0-12.0$ Å^{-1}	imid	Cu−C_2	(3)	[2.97]	0.0023	[−0.19]	⟨0.059⟩	imid	Cu−C_2	(2)	[2.91]	0.0065	[−4.18]	⟨0.076⟩
	imid	Cu−N_3	(3)	[4.11]	[0.0032]	[−0.19]		imid	Cu−N_3	(2)	[4.03]	[0.0091]	[−4.18]	
	imid	Cu−C_4	(3)	[4.14]	[0.0032]	[−0.19]		imid	Cu−C_4	(2)	[4.06]	[0.0091]	[−4.18]	
	imid	Cu−C_5	(3)	[3.01]	[0.0023]	[−0.19]		imid	Cu−C_5	(2)	[2.95]	[0.0066]	[−4.18]	
pig kidney	imid + N/O	Cu−N	(4)	2.00	0.0050	0.80	0.112	imid + N/O	Cu−N	(3)	1.96	0.0070	−2.96	0.128
$k = 2.0-12.0$ Å^{-1}	imid	Cu−C_2	(3)	[3.00]	0.0012	[0.80]	⟨0.071⟩	imid	Cu−C_2	(2)	[2.94]	0.0060	[−2.96]	⟨0.079⟩
	imid	Cu−N_3	(3)	[4.16]	[0.0016]	[0.80]		imid	Cu−N_3	(2)	[4.08]	[0.0083]	[−2.96]	
	imid	Cu−C_4	(3)	[4.18]	[0.0016]	[0.80]		imid	Cu-C_4	(2)	[4.11]	[0.0083]	[−2.96]	
	imid	Cu−C_5	(3)	[3.04]	[0.0012]	[0.80]		imid	Cu−C_5	(2)	[2.98]	[0.0061]	[−2.96]	
bovine plasma	imid + N/O	Cu−N	(4)	1.98	0.0030	−0.67	0.069	imid + N/O	Cu−N	(3)	1.92	0.0068	−5.54	0.102
$k = 2.0-12.0$ Å^{-1}	imid	Cu−C_2	(3)	[2.96]	0.0023	[−0.67]	⟨0.050⟩	imid	Cu−C_2	(2)	[2.88]	0.0065	[−5.54]	⟨0.069⟩
	imid	Cu−N_3	(3)	[4.10]	[0.0032]	[−0.67]		imid	Cu−N_3	(2)	[3.99]	[0.0091]	[−5.54]	
	imid	Cu−C_4	(3)	[4.13]	[0.0032]	[−0.67]		imid	Cu−C_4	(2)	[4.02]	[0.0091]	[−5.54]	
	imid	Cu−C_5	(3)	[3.00]	[0.0023]	[−0.67]		imid	Cu−C_5	(2)	[2.92]	[0.0066]	[−5.54]	
arthrobacter P1	imid + N/O	Cu−N	(4)	1.98	0.0015	0.37	0.064	imid + N/O	Cu−N	(3)	1.99	0.0092	−0.87	0.115
$k = 2.0-12.0$ Å^{-1}	imid	Cu−C_2	(3)	[2.97]	0.0013	[0.37]	⟨0.055⟩	imid	Cu−C_2	(2)	[2.98]	0.0033	[−0.87]	⟨0.086⟩
	imid	Cu−N_3	(3)	[4.12]	[0.0019]	[0.37]		imid	Cu−N_3	(2)	[4.13]	[0.0045]	[−0.87]	
	imid	Cu−C_4	(3)	[4.15]	[0.0019]	[0.37]		imid	Cu−C_4	(2)	[4.15]	[0.0046]	[−0.87]	
	imid	Cu−C_5	(3)	[3.01]	[0.0014]	[0.37]		imid	Cu−C_5	(2)	[3.01]	[0.0033]	[−0.87]	

[a] Group is the chemical unit defined for the multiple scattering calculation. N_s is the number of scatterers (or groups) per metal. R_{as} is the metal-scatterer distance. σ_{as}^2 is a mean square deviation in R_{as}. DE0 is the shift in E_0 for the theoretical scattering functions. [b] f' is normalized error $(\chi^2 f' = \sum_i [k^3(\chi_i^{obs} - \chi_i^{calc})]^2/N\}^{1/2}/[(k^3\chi^{obs})_{max} - (k^3\chi^{obs})_{min}]$. [c] Numbers in angle brackets are f' for the smoothed data. [d] Numbers in parentheses were not varied during optimization. [e] Numbers in square brackets were constrained either to be a multiple of the above value (σ_{as}^2) or to maintain a constant difference (R_{as}).

an excellent model for the Cu(II)-site structures of the other amine oxidases examined here. The coordination and geometry of the Cu(II) site in the *E. coli* amine oxidase (crystallized from citrate)[9] is an equally good model for Cu(II)-site structures in other amine oxidases given the similarities of the PSAO and *E. coli* amine oxidase crystal structures.

Although the EXAFS curve-fitting results for the reduced enzymes are not unequivocal, the fits are consistent with the conclusion from the Cu(I)-edge analysis that the Cu(I) centers in amine oxidases are three-coordinate. Coordination numbers are generally less well-determined by EXAFS curve fitting than distances; the relatively low EXAFS amplitude of the Cu(I)

amine oxidases, which decreases the signal-to-noise, compounds the uncertainty. Moreover, the EXAFS fits may be influenced by static disorder in all the first-shell (N,O) distances, or by dynamic disorder in a specific Cu(I)−N(imidazole) bond. A simple bond-valence-sum (BVS) analysis[29] of the Cu(I)−N distances (Table 2) supports the assignment of three-coordinate geometries for reduced amine oxidases. Following the procedures given by Thorp,[30,31] the BVS values for two, three, and four coordination to Cu(I) are calculated for each value of R_{as} in Table 2 as follows: 0.69−0.83 for two-coordination; 1.03−1.25 for three-coordination; and 1.38−1.66 for four-coordination. Because the BVS value should agree with the copper oxidation state, a three-coordinate geometry is most consistent with the observed bond distances. Thorp has shown that this simple analysis provides remarkably good correlations (or predictions) of oxidation state or coordination geometry in metalloproteins and model complexes.[30,31] Therefore, we conclude that the data for all five amine oxidases are consistent with a decrease in coordination number from five (or, possibly six) to three upon reduction of Cu(II) to Cu(I) by dithionite. The Cu(I) centers are effectively three-coordinate with N,O donors, and may have substantially distorted geometries. At least two histidine imidazoles are Cu(I) ligands. Three-coordinate Cu(I) complexes with heterocyclic N-donor ligands such as imidazole are expected to react rapidly with dioxygen;[15] the dithionite-reduced forms of amine oxidases are, in fact, readily reoxidized by dioxygen. Thus, the XAS-derived structures and the reactivity of the Cu(I) sites in amine oxidases are in accord with the suggested key role of the [Cu(I)−TPQ$^{\bullet}$] semiquinone (**5**, Scheme 1) in catalytic amine oxidation.[32] There is ample precedent among copper-containing metalloproteins for the reactivity of three-coordinate Cu(I) sites with dioxygen.[15,16,33] Three-coordinate Cu(I) centers with predominately histidine imidazole ligands are likely present in the reduced states of dopamine-β-monooxygenase and peptidylglycine α-amidating monooxygenase.[34,35] Binuclear Cu(I) sites with multiple imidazole ligation are known in hemocyanin (reversible oxygen carrier)[35] and tyrosinase (dioxygenase).[37] Substrates are proposed to coordinate to and reduce the coupled [Cu(II)−tyr$^{\bullet}$] unit in the active site of galactose oxidase;[38,39] dissociation of the product aldehyde is suggested to result in a three-coordinate Cu(I) center, which subsequently reacts with dioxygen.[40,41]

Intramolecular electron transfer is required if the Cu(I) semiquinone is a catalytic intermediate (**4** ⇌ **5**, Scheme 1). In order for such a step to be involved in turnover the rate constant must be greater than or equal to the limiting rate constant, i.e., $k_{ET} \geq k_{cat}$. This has been demonstrated for two amine oxidases, from pea seedlings[7] and *Arthrobacter* P1.[8] However, the magnitude of k_{ET} appears to be quite variable: $k_{ET} \simeq 20\,000$ s^{-1} versus $k_{ET} \simeq 70$ s^{-1} for pea seedling amine oxidase and methylamine oxidase from *Arthrobacter* P1, respectively. Several factors can control the rates of intramolecular electron-transfer reactions, the principal ones being redox potential, distance, and re-organization energies. As noted previously, the three-dimensional structures of the pea seedling and the *E. coli* amine oxidases are very similar. Recently the structure of phenethylamine oxidase from *Arthrobacter globiformis* has been solved[42] and it is homologous to the other structures. Moreover, there are substantial sequence homologies among the *E. coli*, *A. globiformis*, and *A.* P1 enzymes, particularly in structurally important regions and the active site. Given the close similarities among the Cu(II)-site structures, and the Cu(I)-site structures established by the EXAFS results, there may be no major differences in the re-organization energies among the amine oxidases considered here. Another indication that re-organization energies may not account for variations in k_{ET} is the lack of correlation between k_{ET} and the change in average bond length ($\Delta r_{av} \equiv R_{as\ (ox)} - R_{as\ (red)}$) upon reduction. From Table 2, $\Delta r_{av} = 0.04$ Å for pea seedling amine oxidase and $\Delta r_{av} = -0.01$ Å for the *Arthrobacter* enzyme, opposite to the reactivity order.

It is worth considering whether other redox-dependent structural changes may be responsible for the differences in k_{ET}. Decreases in the size of the outer-shell (∼3 and ∼4 Å) FT peaks in the Cu(I) forms of the enzymes (Figure 3), as compared to the Cu(II) forms, suggest either the loss of one of the three histidine ligands (Table 2) or a significant increase in the disorder of the Cu(I)−N_{imid} bond lengths. The latter possibility may be quantitatively assessed by comparing σ_{as}^2 values for the outer-shell scatterers of imidazole ligands when three imidazoles are used in simulations of the two redox states (Tables 1 and 2 in Supporting Information). Either interpretation would represent a significant structural change and a resulting contribution to the reorganization energy that could substantially influence k_{ET}. Considering the already large values for σ_{as}^2 for the outer-shell scatterers of imidazole ligands in the Cu(I) sites, even for two-imidazole simulations (Table 2), the first interpretation—loss of one histidine imidazole upon reduction—might be more likely. If this occurs, then higher σ_{as}^2 values for outer-shell scatterers of imidazole ligands in the Cu(I) state (as observed for most amine oxidases in Table 2) would indicate more disorder between the *two* histidine ligands to Cu(I) than among the *three* histidine ligands to Cu(II). The only exception is PSAO: σ_{as}^2 does *not* increase upon reduction (given the loss of one histidine, Table 2) for this enzyme. It is intriguing that PSAO also has the highest value for k_{ET}. Perhaps an increase in the structural disorder of the remaining histidine imidazole ligands in the Cu(I) site influences the reorganizational energy and k_{ET}.

We also note that it is possible that variations in the redox potentials or the effective electron-transfer distance between the

(29) Brown, I. D.; Altermatt, D. *Acta Crystallogr.* **1985**, *B41*, 244−253.
(30) Thorp, H. H. *Inorg. Chem.* **1992**, *31*, 1585−1588.
(31) Liu, W.; Thorp, H. H. *Inorg. Chem.* **1993**, *32*, 4102−4105.
(32) During turnover, reducing equivalents are derived from substrate and transferred to copper from reduced TPQ. Electrons from dithionite may be transferred to copper via TPQ as well because dithionite can reduce TPQ in most amine oxidases. At this time we cannot rule out the possibility that there may be structural differences between the Cu(I) sites in dithionite-reduced versus substrate-reduced amine oxidases. Owing to the reversible redox partition (Scheme 1) the substrate-reduced form is difficult to probe by XAS, especially because the Cu(II) state is favored at low temperatures. The Cu(I) state is stabilized by the addition of cyanide and other exogenous ligands, and structural studies of this complex are underway.
(33) Murthy, N. N.; Karlin, K. D. In *Mechanistic Bioinorganic Chemistry*; Thorp, H. H., Pecoraro, V. L., Eds.; American Chemical Society: Washington, DC 1995; pp 165−193 and references therein.
(34) Blackburn, N. J.; Hasnain, S. S.; Pettingill, T. M.; Strange, R. W. *J. Biol. Chem.* **1991**, *266*, 23120−23127.
(35) Boswell, J. S.; Reedy, B. J.; Kulathila, R.; Merkler, D. J.; Blackburn, N. J. *Biochemistry* **1996**, *35*, 12241−12250.
(36) Hazes, B.; Magnus, K. A.; Bonaventura, C.; Bovaventura, J.; Dauter, Z.; Kalk, K.; Hol, W. G. J. *Protein Sci.* **1993**, *2*, 597−619.
(37) Solomon, E. I.; Baldwin, M. J.; Lowery, M. D. *Chem. Rev.* **1992**, *92*, 521−542 and references therein.
(38) Evidence for substrate coordination is presented in: Knowles, P. F.; Brown, R. D., III; Koenig, S. H.; Wang, S.; Scott, R. A.; McGuirl, M. A.; Brown, D. E.; Dooley, D M. *Inorg. Chem.* **1995**, *34*, 3895−3902.
(39) Clark, K.; Penner-Hahn, J. E.; Whittaker, M. M.; Whittaker, J. W. *J. Am. Chem. Soc.* **1990**, *112*, 6433−6434.
(40) Whittaker, J. W. In *Bioinorganic Chemistry of Copper*; Karlin, K. D., Tyeklár, Z., Eds.; Chapman and Hall: New York, 1993; pp 447−458.
(41) Whittaker, J. W. In *Metal Ions in Biological Systems*; Sigel, H., Sigel, A., Eds.; Dekker: New York, 1994; Vol. 30, pp 315−360.
(42) Wilce, M. C. J.; Dooley, D. M.; Freeman, H. C.; Guss, J. M.; Matsunami, H.; McIntire, W. S.; Ruggiero, C. E.; Tanizawa, K. T.; Yamaguchi, H. *Biochemistry* **1997**, *36*, 16116−16133.

reduced quinone and Cu(II) may control k_{ET}. The crystallographic results suggest that the TPQ residue may adopt multiple conformations within the active site, or be dynamically mobile, or both.[9,10] These issues are currently being investigated.

Acknowledgment. Jun Dong, Hui Zhang, and Shengke Wang are thanked for assistance in XAS data collection. We are grateful to Dr. Christina M. V. Stålhandske for help in the latter stages of XAS data analysis. This research was supported by NIH Grants GM 27659 (D.M.D.) and GM 42025 (R.A.S.). XAS data were collected at the Stanford Synchrotron Radiation Laboratory (SSRL), which is operated by the Department of Energy, Division of Chemical Sciences. The SSRL Biotechnology program is supported by the NIH, Biomedical Resource Technology Program, Division of Research Resources.

Supporting Information Available: A listing of attempted fits of the EXAFS data for oxidized and reduced amine oxidases (17 pages, print/PDF). See any current masthead page for ordering information and Web access instructions.

JA970312A